# Computational Study on the Mechanisms and Energetics of Trimethylindium Reactions with $H_2O$ and $H_2S$

**P. Raghunath[†] and M. C. Lin*[,†,‡]**

*Center for Interdisciplinary Molecular Science, Institute of Molecular Science, National Chiao Tung University, Hsinchu 300, Taiwan, Department of Chemistry, Emory University, Atlanta, Georgia 30322*

*Received: November 20, 2006; In Final Form: April 26, 2007*

The reactions of trimethylindium (TMIn) with $H_2O$ and $H_2S$ are relevant to the chemical vapor deposition of indium oxide and indium sulfide thin films. The mechanisms and energetics of these reactions in the gas phase have been investigated by density functional theory and ab initio calculations using the CCSD(T)/[6-31G(d,p)+Lanl2dz]//B3LYP/[6-31G(d,p)+Lanl2dz] and CCSD(T)/[6-31G(d,p) + Lanl2dz] //MP2/[6-31G-(d,p)+Lanl2dz] methods. The results of both methods are in good agreement for the optimized geometries and relative energies. When TMIn reacts with $H_2O$ and $H_2S$, initial molecular complexes [$(CH_3)_3$In:$OH_2$ (**R1**)] and [$(CH_3)_3$In:$SH_2$ (**R2**)] are formed with 12.6 and 3.9 kcal/mol binding energies. Elimination of a $CH_4$ molecule from each complex occurs with a similar energy barrier at TS1 (19.9 kcal/mol) and at TS3 (22.1 kcal/mol), respectively, giving stable intermediates $(CH_3)_2$InOH and $(CH_3)_2$InSH. The elimination of the second $CH_4$ molecule from these intermediate products, however, has to overcome very high and much different barriers of 66.1 and 53.2 kcal/mol, respectively. In the case of DMIn with $H_2O$ and $H_2S$ reactions, formation of both InO and InS is exothermic by 3.1 and 30.8 kcal/mol respectively. On the basis of the predicted heats of formation of **R1** and **R2** at 0 K and −20.1 and 43.6 kcal/mol, the heats of formation of $(CH_3)_2$InOH, $(CH_3)_2$InSH, $CH_3$InO, $CH_3$InS, InO, and InS are estimated to be −20.6, 31.8, and 29.0 and 48.4, 35.5, and 58.5 kcal/mol, respectively. The values for InO and InS are in good agreement with available experimental data. A similar study on the reactions of $(CH_3)_2$In with $H_2O$ and $H_2S$ has been carried out; in these reactions $CH_3$InOH and $CH_3$InSH were found to be the key intermediate products.

## Introduction

The Group III−VI materials such as indium oxide and indium sulfide are wide-gap semiconductor materials which have been the subject of significant interest, due to their potential uses in photovoltaic or optoelectronic applications.[1−5] Indium sulfides are mid-band gap semiconductors that exist in a number of forms with band gaps ranging from 1.9 to 2.45 eV.[6] Indium monosulfide film exhibits the absorption coefficient of an order of $10^5$ $cm^{-1}$ and the energy band gap of 1.94 eV. These properties are suitable for solar cells.[6b]

The spectroscopic and thermodynamic data of InO and InS have not been well characterized. Spectrum of indium oxide was reported by Watson and Shambon.[7] Burns et at., employing Knudsen cell-mass spectrometric techniques, identified the molecule InO, but the intensity was too small to measure.[8] There are two known oxides of indium; they are monoxide (InO) and sesquioxide ($In_2O_3$). The monoxide is black and probably not as stable; on further oxidation, the monoxide becomes sesquioxide, which is very stable, and volatilizes without decomposition at 1123 K.[9] Indium oxide is an insulator in its stoichiometric form, whereas in its nonstoichiometric form it behaves as a highly conducting semiconductor with a wide direct optical band gap (3−4 eV) providing high transparency in the visible region and high reflectivity in the infrared (IR) region. This unique combination of electrical and optical properties has led numerous researchers to investigate thoroughly about the growth and characterization of thin semiconducting indium oxide films due to their obvious application as transparent conductive electrodes in optoelectronic devices, such as solar cells.[10]

Our study was motivated by our own InN/$TiO_2$ nanoparticle solar cell fabrication process in which the deposition of InS between InN and $TiO_2$ nanoparticles using TMIn and $H_2S$ was found to enhance InN/$TiO_2$ system's photoefficiency (unpublished work). Accordingly, we tried to understand the chemical linking of the InN and $TiO_2$ with InS. The reaction of TMIn and $H_2S$ on $TiO_2$ will be studied and compared with the gas-phase results presented in this paper in the near future.

On considering the importance of the indium oxide and indium sulfide, we have carried out the detailed potential energy surface (PES) studies using high level ab initio and DFT calculations on trimethyIndium $(CH_3)_3$In(TMIn) when reacted with $H_2O$ and $H_2S$. These studies explore the stability and the structural properties of the various possible species, which we believe could help in predictions of the formation of InO and InS on semiconductor surfaces or in the bulk states. In addition, transition states connecting isomers have also been located to assess the rearrangement barriers. The calculated geometries, IR frequencies, and heats of formation could be helpful for the likely identification of the species in the laboratory.

## Computational Methods

Recent work on indium metal complexes has shown that the widely used B3LYP and MP2 methods with Lanl2dz basis sets are quite suitable for geometry and property predictions.[11] We have carried out the geometry optimization of all the reactants,

* Corresponding author. E-mail: chemmcl@emory.edu.
[†] National Chiao Tung University.
[‡] Emory University.

10.1021/jp0677142 CCC: $37.00 
Published on Web 06/23/2007

**TABLE 1: Relative Energies[a] (kcal/mol) of Various Species in the $(CH_3)_3In + H_2O$ Reaction Calculated at the Different Levels**

| species | B3LYP/ [6-31G(d,p)/Lanl2dz] | MP2/[6-31G(d,p)/ Lanl2dz] | CCSD(T)/[6-31G(d,p)/Lanl2dz] //B3LYP/[6-31G(d,p)/Lanl2dz] | CCSD(T)/[6-31G(d,p)/Lanl2dz] //MP2/[6-31G(d,p)/Lanl2dz] |
|---|---|---|---|---|
| $^1(CH_3)_3In + {}^1H_2O$ | 0.0 | 0.0 | 0.0 (0.0)[b] | 0.0 |
| $^1(CH_3)_3In{:}OH_2$ (**R1**) | −12.4 | −12.9 | −12.6 (−13.1) | −12.6 |
| TS1 | 2.8 | 5.0 | 7.3 (7.1) | 7.4 |
| $TS2 + CH_4$ | 34.5 | 35.4 | 39.4 (45.0) | 39.5 |
| $^1(CH_3)_2InOH + CH_4$ | −27.4 | −27.9 | −26.7 (−23.3) | −26.6 |
| $^1CH_3InO + 2CH_4$ | 9.4 | 2.9 | 7.6 (16.8) | 7.7 |
| $^2InO + 2CH_4 + CH_3$ | 62.1 | 66.1 | 55.6 (56.5) | 55.9 |

[a] Energies are ZPVE-corrected. [b] The relative energies are calculated using CCSD(T)/[6-31G(d,p)/SDD]//B3LYP/[6-31G(d,p)/Lanl2dz] level values are given in the parentheses.

products, transition states, and intermediate molecules in their ground state configurations using the Gaussian 03 program.[12] Optimizations are carried out on all of the possible reactions of TMIn and DMIn with $H_2O$ and $H_2S$ by the B3LYP and MP2 methods. The B3LYP method consists of Becke's three-parameter hybrid exchange function combined with the Lee−Yang−Parr correlation function.[13] The basis set used in this paper is Lanl2dz, which includes the D95 double-$\xi$ basis set for In along with Hay and Wadt's effective core potential (ECP)[14] and the 6-31G(d,p) basis set for main group elements. All the geometries are analyzed by harmonic vibrational frequencies obtained at the same level and characterized as minima (no imaginary frequency) or as a transition state (one imaginary frequency). Transition state geometries are then used as an input for IRC calculations to verify the connectivity of the reactants and products.[15] The higher-order correlation energy correction of the both B3LYP and MP2 energies were obtained at the single point using the CCSD(T)/[6-31G(d,p)+Lanl2dz] method.[16a−d] Although Dunning and Hay ECP basis set (Lanl2dz) is quite effective, the method is old. Therefore, the more recent Stuttgart/Dresden relativistic effective core potential (ECP) is employed for the In atom which represents the reaction center of the systems.[17] All the relative energies in the tables have been corrected for zero-point vibrational energies (ZPVE, unscaled). The effect of basis set superposition error (BSSE) has been estimated by the standard function counterpoise (CP) method.[16e] Spin contamination was not high as was judged by the expectation values of $\langle S^2 \rangle$ (InO = 0.76, InS = 0.75, and $CH_3$ = 0.75).

## Results and Discussions

**Potential Energy Surfaces and Reaction Mechanism.** *Reactions of Trimethylindium $(CH_3)_3In$ with $H_2O$.* To validate the accuracy of the theoretical method chosen in this study, we first consider the formation of InO when trimethyl indium reacts with $H_2O$. We have carried out calculations for all the reaction steps using two different methodologies, namely B3LYP and MP2. The resulting amount of data turned out to be large. Hence, for clarity the details of all the relative energies of the gas-phase reactants, intermediates, products, and transition states are listed in Table 1 and the geometrical parameters obtained by both B3LYP/[6-31G(d,p)+Lanl2dz] and MP2/[6-31G-(d,p)+Lanl2dz] methods are given in Figure 1. Along with we have repeated all the single point calculations at the B3LYP level in conjunction with the Stuttgart/Dresden ECP and associated triple-$\xi$ SDD basis set for In and 6-31G(d,p) basis for main group elements. The potential energy diagram obtained at the CCSD(T)/[6-31G(d,p)+LanL2dz]//B3LYP/[6-31G(d,p) +LanL2dz] level of theory is presented in Figure 2. The relative energies are calculated with respect to the reactants of $In(CH_3)_3 + H_2O$.

Trimethyl indium has a planar structure, and the bond length of In−C is 2.163 Å with low-energy rotational barriers for the methyl groups. The association reaction of the electron deficient $In(CH_3)_3$ and $H_2O$ can form a molecular complex, i.e., $[(CH_3)_3$-$In{:}OH_2$ (**R1**)] as shown in Figure 1. Complexation with a molecule of water yields a most stable complex structure, **R1**, which lies 12.4 kcal/mol and 12.9 kcal/mol below the reactants calculated at the B3LYP/[6-31G(d,p)+LanL2dz] and MP2/[6-31G(d,p) + lanl2dz] methods, respectively. The predicted value is 12.6 kcal/mol, by both CCSD(T)//B3LYP and CCSD(T)// MP2 methods. As shown in the Figure 1, water is located with oxygen pointing toward the In atom in the top and middle of molecule at a distance of 2.375 Å (2.374 Å by MP2). The complex has $C_1$ symmetry, and the C−In−C angle has changed from 120° to 119.6°. Formation of the second complex, one of the H atom of water interacts with one of the $CH_3$ of TMIn, $(CH_3)_2InCH_3{:}HOH$ is very weak and unstable in both methods.

The decomposition of **R1** to the most stable intermediate $(CH_3)_2InOH$ and a $CH_4$ molecule requires the transition state energy at **TS1** of around 19.9 kcal/mol (or 7.3 kcal/mol above the reactants). The transition vector is dominated by the motion of hydrogen, which is 1.205 Å from the oxygen and 1.465 Å from the carbon. The In−O bond is almost formed (2.137 vs 1.927 Å $(CH_3)_2InOH$). The In−C bond is substantially elongated to 2.435 Å from 2.163 Å in $(CH_3)_3In$. On the basis of the CCSD-(T)/[6-31G(d,p)+LanL2dz]//B3LYP/[6-31G(d,p)+LanL2dz] level of calculation, the formation of the $(CH_3)_2InOH + CH_4$ products is found to be most exothermic 26.7 kcal/mol. Calculations from the MP2 method also confirm the result with 26.6 kcal/mol exothermicity. Geometrical parameter of the $(CH_3)_2InOH$ structure in terms of bond length between the In−O is 1.927 Å and In−C is 2.153 Å.

The decomposition of the $(CH_3)_2InOH$ product to $CH_3InO + CH_4$ requires 66.1 kcal/mol of energy; the decomposition takes place via the transition state (TS2) with O−H and In−C bond lengths of 1.330 Å and 2.525 Å respectively. TS2 is very similar to TS1, located at 34.5 kcal/mol and 35.4 kcal/mol above the association complex of $TMIn + H_2O$ reactants calculated using the B3LYP/[6-31G(d,p)+LanL2dz] and MP2/[6-31G-(d,p)+Lanl2dz] level respectively. The CCSD(T) energy calculated with both B3LYP and MP2 optimized geometries essentially the same around 39 kcal/mol.

In this potential energy surface, the reaction channel producing $CH_3InO + 2CH_4$ is only 7.6 kcal/mol above the reactants. Further decomposition of $CH_3InO$ produces the doublet radicals of InO and $CH_3$. In this process, breaking of $CH_3$ from indium requires 48.0 kcal/mol of endothermic energy predicted at the CCSD(T)//B3LYP level of theory. The doublet ground electronic state of In−O has a bond length of 2.023 Å, which is longer than that in $CH_3In$−O, 1.769 Å.

*Reactions of Trimethylindium $(CH_3)_3In$ with $H_2S$.* In this section, we describe in detail the mechanism for the analogous $H_2S$ reaction along the PES's and try to underline the similarities and differences between the two ligands. The calculated structures of intermediates, transition states and products of all

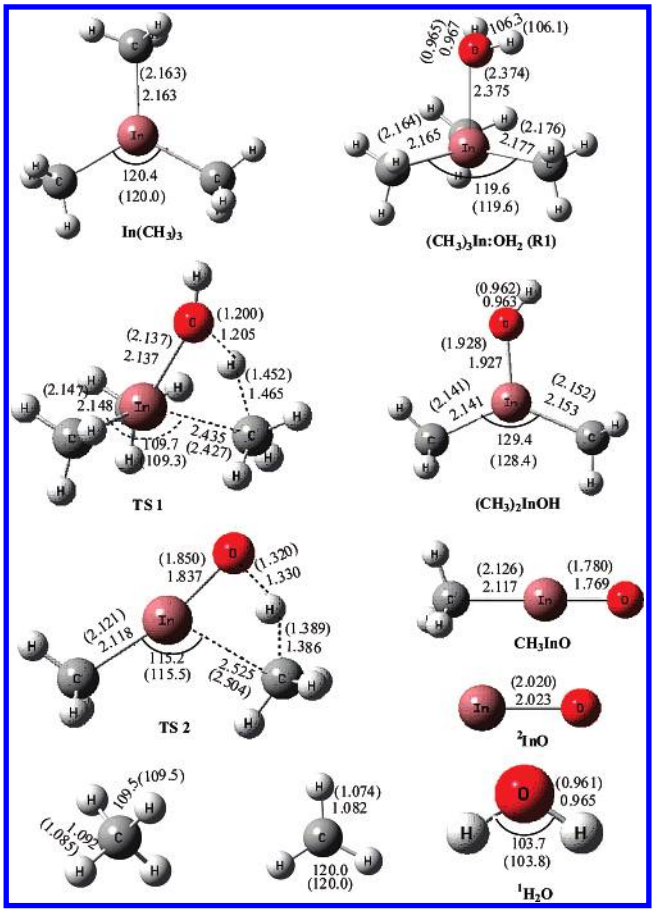


**Figure 1.** All the optimized geometries of intermediates and transition states are calculated using B3LYP/[6-31G(d,p)+Lanl2dz] level, and MP2 values are given in the parentheses. Bond lengths are in angstroms, and angles in degrees.

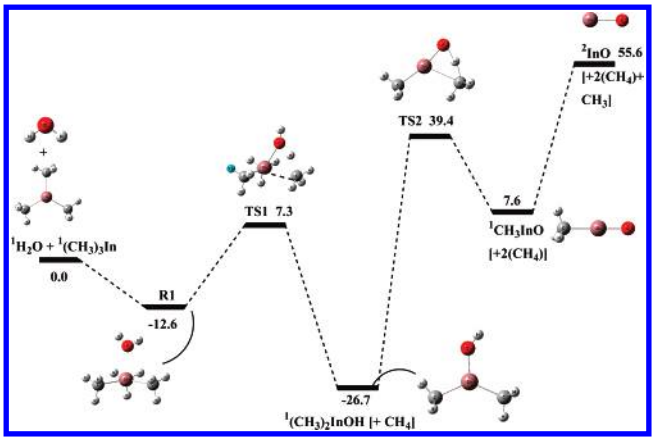


**Figure 2.** Potential energy surface of the $H_2O$ + TMIn reaction. Relative energies (kcal/mol) calculated using the CCSD(T)/[6-31G-(d,p)+Lanl2dz]//B3LYP/[6-31G(d,p)+Lanl2dz] + ZPVE levels of theory.

investigated reactions are given in Figure 3 and relative energies are given in Table 2. The potential energy surface has been studied at the CCSD(T)/[6-31G(d,p)+LanL2dz]//B3LYP/[6-31G(d,p)+LanL2dz] level of theory and is presented in Figure 4. The predicted moments of inertia and vibrational frequencies for all these species are summarized in Supporting Information Table S1. The relative energies are calculated with respect to the reactants, $In(CH_3)_3$ + $H_2S$.

The gas-phase association reaction of trimethylindium with hydrogen sulfide can give rise to molecular complex, $(CH_3)_3$-$In:SH_2$ (**R2**) without intrinsic barriers. Formation of the **R2** is

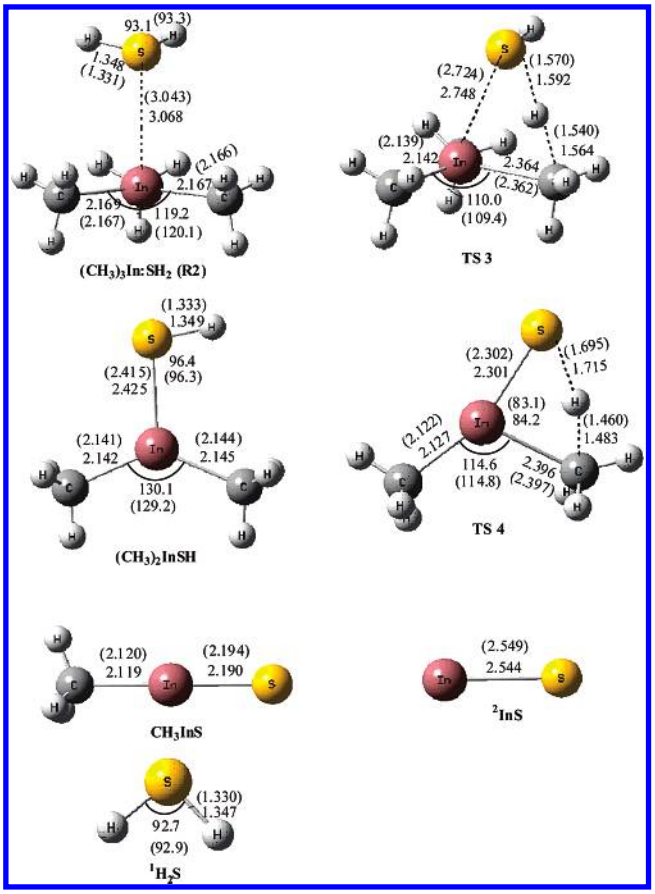


**Figure 3.** All the optimized geometries of intermediates and transition states are calculated using B3LYP/[6-31G(d,p)+Lanl2dz], and MP2 values are given in the parentheses. Bond lengths are in angstroms, and angles in degrees.

less exothermic when compared to **R1** and has a value 3.9 kcal/mol below the reactants. First step in this reaction is sulfur atom interacting with indium of $In(CH_3)_3$ to give the **R2** complex. The bond length of In−S is 3.068 and 3.043 Å calculated at the B3LYP/[6-31G(d,p)+LanL2dz] and MP2/[6-31G-(d,p)+Lanl2dz] levels, respectively. The hydrogen-bonding energy between the $CH_3$ group and a hydrogen atom of the $H_2S$ molecule was found to be unstable.

Complex **R2**, $(CH_3)_3In:SH_2$ can decompose to give $(CH_3)_2$-InSH + $CH_4$ by a cyclic transition state. This reaction channel is predicted to have a potential barrier of 22.1 kcal/mol, which may be compared with the value of 15.4 kcal/mol by B3LYP and 20.2 kcal/mol by the MP2 method. The exothermicity of the process is predicted to be 29.0 kcal/mol. The transition state (TS3) of this channel is nonplanar, and the reaction takes place with the formation of the In−S bond with a bond length of 2.748 Å and those of S−H and C−H, 1.592 and 1.564 Å, respectively. The bond length of In−C elongates from 2.163 Å in TMIn to 2.364 Å.

The intermediate product $(CH_3)_2InSH$ has the In−S bond length 2.425 Å and In−C bond length 2.145 Å according to the B3LYP method; these values may be compared with 2.415 and 2.144 Å obtained by the MP2 method. From the $(CH_3)_2$-InSH, the reaction proceeds by the migration of a hydrogen atom from S to C to eliminate $CH_4$ and the $CH_3InS$ product via transition state TS4. The barrier height of this reaction is about 53.2 kcal/mol, which may be compared with the values 47.6 kcal/mol and 52.1 kcal/mol calculated at B3LYP and MP2 methods, respectively. In this PES, the formation of products $CH_3InS$ + $2CH_4$ is most exothermic with 22.3 kcal/mol

**TABLE 2: Relative Energies[a] (kcal/mol) of Various Species in the $(CH_3)_3In + H_2S$ Reaction Calculated at the Different Levels**

| species | B3LYP/ [6-31G(d,p)/Lanl2dz] | MP2/[6-31G(d,p)/ Lanl2dz] | CCSD(T)/[6-31G(d,p)/Lanl2dz] //B3LYP/[6-31G(d,p)/Lanl2dz] | CCSD(T)/[6-31G(d,p)/Lanl2dz] //MP2/[6-31G(d,p)/Lanl2dz] |
|---|---|---|---|---|
| $^1(CH_3)_3In + {}^1H_2S$ | 0.0 | 0.0 | 0.0 (0.0)[b] | 0.0 |
| $^1(CH_3)_3In{:}SH_2$ (**R2**) | −1.8 | −3.8 | −3.9 (−3.9) | −3.8 |
| TS3 | 13.6 | 16.4 | 18.2 (17.3) | 18.1 |
| $TS4 + CH_4$ | 17.7 | 22.5 | 24.2 (23.3) | 24.2 |
| $^1(CH_3)_2InSH + CH_4$ | −29.9 | −29.6 | −29.0 (−29.4) | −28.9 |
| $^1CH_3InS + 2CH_4$ | −22.7 | −22.0 | −22.3 (−22.5) | −22.2 |
| $^2InS + 2CH_4 + CH_3$ | 33.9 | 34.1 | 27.9 (32.1) | 28.1 |

[a] Energies are ZPVE-corrected. [b] The relative energies are calculated using CCSD(T)/[6-31G(d,p)/SDD] //B3LYP/[6-31G(d,p)/Lanl2dz] level values are given in the parentheses.

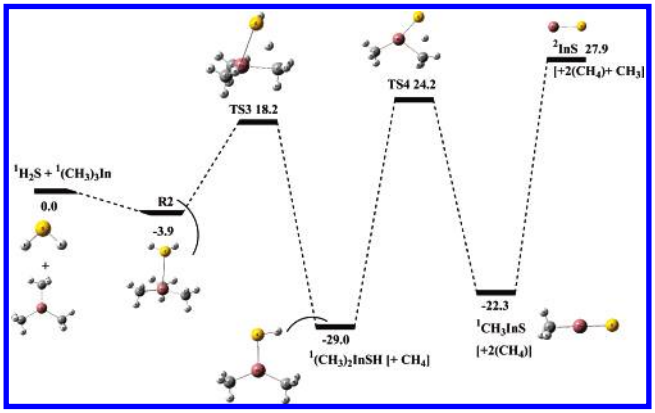


**Figure 4.** Potential energy surface of the $H_2S$ + TMIn reaction. Relative energies (kcal/mol) calculated using the CCSD(T)/[6-31G-(d,p)+Lanl2dz]//B3LYP/[6-31G(d,p)+Lanl2dz] + ZPVE levels of theory.

exothermicity. In the $In(CH_3)_3 + H_2S$ reaction channel, the two intermediate products $(CH_3)_2InSH + CH_4$ and $CH_3InS + 2CH_4$ have exothermic energy difference is around 6.5 kcal/mol.

$CH_3InS$ has $C_{3V}$ symmetry with the In−S and In−C bond lengths predicted to be 2.190 and 2.119 Å, respectively. Finally the dissociation of the most stable intermediate $CH_3InS$ to doublet InS and $CH_3$ radicals is highly endothermic (50.2 kcal/mol). The final reaction product of this PES is $InS + 2CH_4 + CH_3$ which is around 33.9 kcal/mol above the reactants predicted by B3LYP method and 34.1 kcal/mol by the MP2 method. Here the energy difference between the two methods is 0.2 kcal/mol. In the quartet state of diatomic InS and InO, their bonds are very long and unstable. The InO and InS molecules have doublet ground state bond lengths of 2.023 Å (2.020 Å) and 2.544 Å (2.549 Å), respectively, calculated by B3LYP (MP2) methods.

The gas-phase association reaction of trimethylindium with $H_2O$ and $H_2S$ can give rise to molecular complexes, $(CH_3)_3In{:}OH_2$ R1 and $(CH_3)_3In{:}SH_2$ R2. The basis set superposition error (BSSE) correction was calculated with a complete counterpoise procedure for each of the basis sets are given in the Supporting Information Table S2.

When the two potential energy surfaces of TMIn reactions with $H_2O$ and $H_2S$ are compared, the initial molecular complex [$(CH_3)_3In{:}OH_2$ (**R1**)] is 8.7 kcal/mol more stable than [$(CH_3)_3In{:}SH_2$ (**R2**)]. Their decomposition reactions give the intermediate products $(CH_3)_2InOH$ and $(CH_3)_2InSH$, both having about same energy (TS1 is 19.9 kcal/mol and TS3 is 22.1 kcal/mol with the CCSD(T)//B3LYP method). Surprisingly, in the case of $CH_3InO$, its formation by elimination of $2CH_4$ is endothermic by 7.6 kcal/mol, whereas the similarly formed product $CH_3InS$ is 22.3 kcal/mol exothermic. Required energies for the final unimolecular dissociation giving both InO and InS are 48.0 and 50.2 kcal/mol, respectively. Overall, both DFT and ab initio methods with the correlation energy correction seem to have good agreement in geometries and relative energies. The overall reaction mechanism for these reactants can be written as follows (X = O, S):

$$(CH_3)_3In + XH_2 \rightarrow (CH_3)_3In{:}XH_2 \quad (1)$$

$$(CH_3)_3In{:}XH_2 \rightarrow (CH_3)_2InXH + CH_4 \quad (2)$$

$$(CH_3)_2InXH \rightarrow (CH_3)InX + 2CH_4 \quad (3)$$

$$(CH_3)InX \rightarrow InX + 2CH_4 + CH_3 \quad (4)$$

**Decomposition of TMIn and Reactions of DMIn with $H_2O$ and $H_2S$.** Under some experimental CVD conditions, for example, that carried out in a heated reactor, the decomposition of TMIn may take place. The experimental dissociation energy of first $CH_3$−In bond of TMIn has been reported to be 49 ± 7 kcal/mol using the toluene carrier-gas technique at 6−34 Torr pressure.[18a,b] This value is lower than those predicted by the B3LYP/6-31(G(d,p)+Lanl2dz and CCSD(T)//B3LYP methods, 61.3, and 62.4 kcal/mol. The lower experimental value may be attributed to the combination of the incomplete radical scavenging by toluene and the low-pressure employed the well-known drawbacks of the toluene carrier gas technique. The $(CH_3)_2In$, DMIn, formed in the decomposition reaction, can react with $H_2O$ and $H_2S$. We thus also investigate their reaction mechanisms in this work. The geometries of all species involved in the reactions using the B3LYP method are depicted in Figure 5. The predicted energies with both B3LYP and MP2 methods are summarized in Table 3 and 4. The potential energy diagrams obtained at the CCSD(T)/[6-31G(d,p)+Lanl2dz]//B3LYP/[6-31G(d,p)+Lanl2dz] level of theory is presented in Figure 6 and 7.

As shown in Figure 6 and 7, the reactions of DMIn with $H_2O$ and $H_2S$ can form molecular complexes $(CH_3)_2In{:}OH_2$ **R3** and $(CH_3)_2In{:}SH_2$ **R4**. In the initial steps, the O and S atoms in the $H_2O$ and $H_2S$ can directly associate with the indium atom in $In(CH_3)_2$ by a barrierless process forms with **R3** and **R4**, their exothermic energy around 8.4 and 2.0 kcal/mol respectively at the CCSD(T)/[6-31G(d,p)+Lanl2dz]//B3LYP/[6-31G(d,p)+Lanl2dz] level. As shown in the Figure 5 bond length between the In−O and In−S are 2.432 Å and 3.173 Å respectively. In the next reaction step, the molecular complexes **R3** and **R4**, the H atom of the $H_2O$ and $H_2S$ can react with one of the methyl groups intramolecularly to eliminate $CH_4$, producing $CH_3InOH$ and $CH_3InSH$ via TS5 and TS7 respectively. This $CH_4$ elimination **R3** is predicted to have a low potential barrier (TS5) of 18.9 kcal/mol with an exothermicity of 17.6 kcal/mol. For the similar decomposition of **R4**, a 20.8 kcal/mol energy is required to eliminate the $CH_4$ to form $CH_3InSH$ with 27.6 kcal/mol exothermicity from the **R4** complex.

Interestingly, in the DMIn + $H_2O$ reaction channel, migration of the $CH_3$ group in $CH_3InOH$ takes place through an 11.9 kcal/mol barrier at TS6 to form an unusual $InOH{:}CH_3$ complex lying

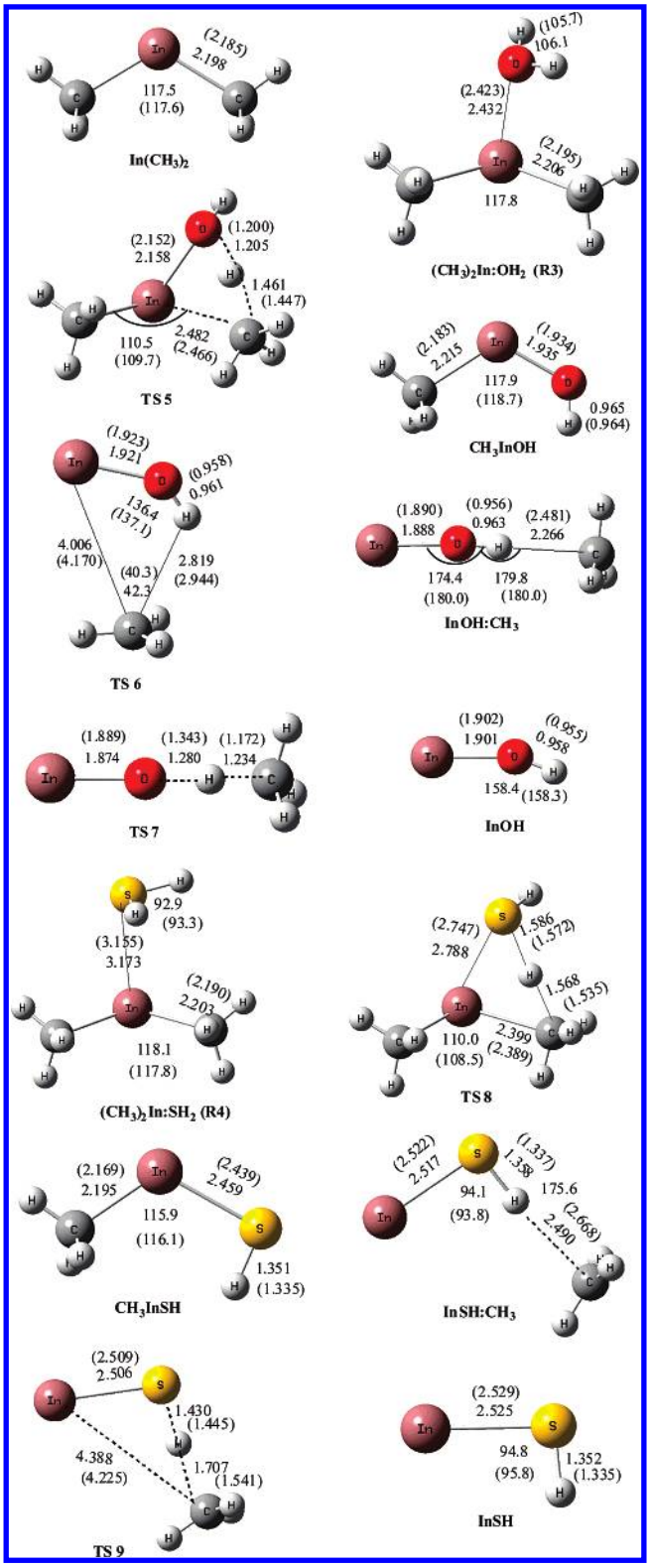


**Figure 5.** All the optimized geometries of intermediates and transition states are calculated using B3LYP/[6-31G(d,p)+Lanl2dz], and MP2 values are given in the parentheses. Bond lengths are in angstroms, and angles in degrees.

11.4 kcal/mol above $CH_3InOH + CH_4$. Further decomposition of $InOH:CH_3$ giving InO and $CH_4$ through an 18.3 kcal/mol barrier; the process is 11.5 kcal/mol endothermic from the complex. H dissociation from the most stable intermediate MInOH to MInO requires 75.2 kcal/mol energy.

The PES of the analogous DMIn + $H_2S$ reaction is shown in Figure 7; the formation of InS may proceed by two pathways;

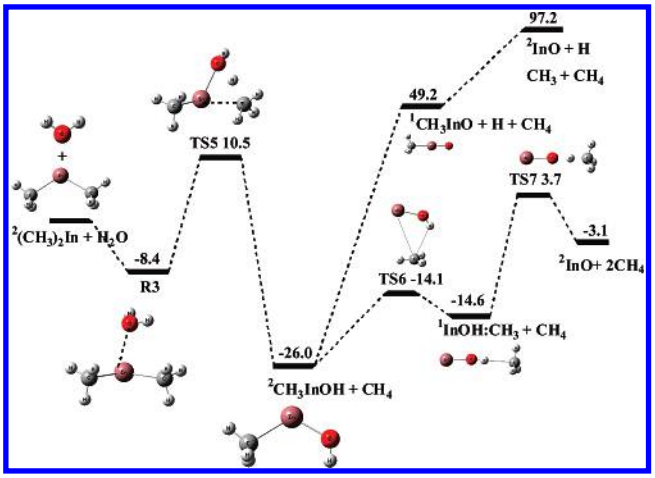


**Figure 6.** Potential energy surface of the $H_2O$ + DMIn reaction. Relative energies (kcal/mol) calculated using the CCSD(T)/[6-31G-(d,p)+Lanl2dz]//B3LYP/[6-31G(d,p)+Lanl2dz] + ZPVE levels of theory.

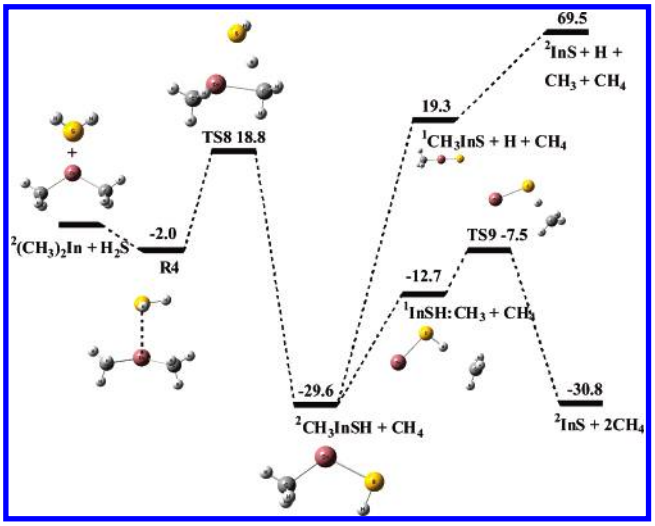


**Figure 7.** Potential energy surface of the $H_2S$ + DMIn reaction. Relative energies (kcal/mol) calculated using the CCSD(T)/[6-31G-(d,p)+Lanl2dz]//B3LYP/[6-31G(d,p)+Lanl2dz] + ZPVE levels of theory.

first the elimination of $CH_4$ from the $CH_3InSH$ was found to occur via the $InSH:CH_3$ complex without a distinct transition state; the complex lies 16.9 kcal/mol above the $CH_3InSH$. The formation of InS by the $CH_4$ elimination process goes through a 5.2 kcal/mol barrier at TS9 with 18.1 kcal/mol exotherimicity. The second pathway is a unimolecular decomposition process of the $CH_3InSH$ produces $CH_3InS$ and H. This process, breaking of H from sulfur requires 50.5 kcal/mol predicted at B3LYP/[6-31G(d,p)+Lanl2dz] and 48.9 kcal/mol energy at the CCSD-(T)//B3LYP level. Similarly, the endothermicity for the dissociation reaction $CH_3InS \rightarrow InS + CH_3$ requires 50.2 kcal/mol, which is quite close to that predicted for the analogous $CH_3$-InO reaction, 48.0 kcal/mol (see Figure. 6).

**Heats of Formation.** The heats of formation of most species involved in the two systems are not known except InO and InS. The predicted heats of formation including InO and InS presented in Table 5 were based on the energies computed at the CCSD(T)/Lanl2dz//B3LYP/Lanl2dz and CCSD(T)/[6-31G-(d,p)]+Lanl2dz//B3LYP/[6-31G(d,p)+Lanl2dz] level. The heats of formation of $(CH_3)_3In:OH_2$ (**R1**)and $(CH_3)_3In:SH_2$ (**R2**) were determined by combining the computed heat of reaction ($\Delta_r H_0^\circ$) from reaction (**1**) with experimental $\Delta_f H_0^\circ$ (0 K) values for $(CH_3)_3In$ (52.97 kcal/mol), $H_2O$ (−57.12 kcal/mol) and $H_2S$

**TABLE 3: Relative Energies[a] (kcal/mol) of Various Species in the $(CH_3)_2In + H_2O$ Reaction Calculated at the Different Levels**

| species | B3LYP/ [6-31G(d,p)/Lanl2dz] | MP2/[6-31G(d,p)/ Lanl2dz] | CCSD(T)/[6-31G(d,p)/Lanl2dz] //B3LYP/[6-31G(d,p)/Lanl2dz] | CCSD(T)/[6-31G(d,p)/Lanl2dz] //MP2/[6-31G(d,p)/Lanl2dz] |
|---|---|---|---|---|
| $^2(CH_3)_2In + {}^1H_2O$ | 0.0 | 0.0 | 0.0 (0.0) | 0.0 |
| $^2(CH_3)_2In-OH_2$ (**R3**) | −9.2 | −10.2 | −8.4 (−8.8) | −9.5 |
| TS5 | 5.2 | 8.1 | 10.5 (10.1) | 10.4 |
| $^2CH_3InOH + CH_4$ | −26.6 | −27.1 | −26.0 (22.8) | −25.8 |
| $TS6 + CH_4$ | −11.3 | −11.9 | −14.1 (−11.4) | −14.7 |
| $^1InOH{:}CH_3 + CH_4$ | −12.4 | −12.5 | −14.6 (−10.7) | −15.3 |
| $TS7 + CH_4$ | 1.9 | 12.6 | 3.7 (7.8) | 2.9 |
| $^2InO + 2CH_4$ | 0.8 | 5.1 | −3.1 (−2.6) | −3.1 |
| $^1CH_3InO + H + CH_4$ | 52.0 | 41.0 | 49.2 (57.9) | 48.8 |
| $^2InO + H + CH_3 + CH_4$ | 104.7 | 104.2 | 97.2 (97.7) | 96.9 |

[a] Energies are ZPVE-corrected.

**TABLE 4: Relative Energies[a] (kcal/mol) of Various Species in the $(CH_3)_2In + H_2S$ Reaction Calculated at the Different Levels**

| species | B3LYP/ [6-31G(d,p)/Lanl2dz] | MP2/[6-31G(d,p)/ Lanl2dz] | CCSD(T)/[6-31G(d,p)/Lanl2dz] //B3LYP/[6-31G(d,p)/Lanl2dz] | CCSD(T)/[6-31G(d,p)/Lanl2dz] //MP2/[6-31G(d,p)/Lanl2dz] |
|---|---|---|---|---|
| $^2(CH_3)_2In + {}^1H_2S$ | 0.0 | 0.0 | 0.0 (0.0) | 0.0 |
| $^2(CH_3)_2In-S\,H_2$ (**R4**) | −0.8 | −2.3 | −2.0 (−1.9) | −2.0 |
| TS8 | 13.8 | 17.1 | 18.8 (18.5) | 18.8 |
| $^2CH_3InSH + CH_4$ | −30.6 | −29.9 | −29.6 (−29.8) | −29.4 |
| $^1InSH{:}CH_3 + CH_4$ | −10.3 | −9.5 | −12.7 (−13.5) | −13.3 |
| $TS9 + CH_4$ | −8.9 | −3.1 | −7.5 (−8.2) | −7.5 |
| $^2InS + 2CH_4$ | −27.5 | −26.9 | −30.8 (−27.0) | −30.9 |
| $^1CH_3InS + H + CH_4$ | 19.9 | 16.0 | 19.3 (18.7) | 18.9 |
| $^2InS + H + CH_3 + CH_4$ | 76.4 | 72.2 | 69.5 (73.3) | 69.1 |

[a] Energies are ZPVE-corrected.

**TABLE 5: Heats of Reaction ($\Delta_r H_0^\circ$) and Heats of Formation ($\Delta_f H_0^\circ$) of Species at 0 K Predicted at the B3LYP/Lanl2dz and CCSD(T)/[6-31G(d,p)+Lanl2dz]//B3LYP/[6-31G(d,p)+Lanl2dz] Level of Theory[a] are Given in Kcal/mol**

| species | $H_2O$ + TMIn reaction[b] | heat of reaction $\Delta_r H_0^\circ$ (kcal/mol) I | heat of reaction $\Delta_r H_0^\circ$ (kcal/mol) II | heat of formation $\Delta_f H_0^\circ$ (kcal/mol) I | heat of formation $\Delta_f H_0^\circ$ (kcal/mol) II |
|---|---|---|---|---|---|
| **R1** | $H_2O + (CH_3)_3In \rightarrow$ **R1** ($(CH_3)_3In{:}OH$) | −16.0 | −12.6 | −20.1 | −16.8 |
| $(CH_3)_2InOH$ | **R1** $\rightarrow (CH_3)_2InOH + CH_4$ | −16.5 | −14.1 | −20.6 | −14.9 |
| $CH_3InO$ | $(CH_3)_2InOH$ $(CH_3)_2InOH \rightarrow CH_3InO + CH_4$ | 33.7 | 34.3 | 29.0 | 35.4 |
| InO | $CH_3InO \rightarrow InO + CH_3$ | 42.1 | 48.0 | 35.5 | 47.5 |

| species | $H_2S$ + TMIn reaction | heat of reaction $\Delta_r H_0^\circ$ (kcal/mol) I | heat of reaction $\Delta_r H_0^\circ$ (kcal/mol) II | heat of formation $\Delta_f H_0^\circ$ (kcal/mol) I | heat of formation $\Delta_f H_0^\circ$ (kcal/mol) II |
|---|---|---|---|---|---|
| **R2** | $H_2S + (CH_3)_3In \rightarrow$ R2 ($(CH_3)_3In{:}SH$) | −5.2 | −3.9 | 43.6 | 44.9 |
| $(CH_3)_2InSH$ | **R1** $\rightarrow (CH_3)_2InSH + CH_4$ | −27.8 | −25.2 | 31.8 | 35.7 |
| $CH_3InS$ | $(CH_3)InSH \rightarrow CH_3InS + CH_4$ | 0.6 | 6.7 | 48.4 | 58.4 |
| InS | $CH_3InS \rightarrow InS + CH_3$ | 45.7 | 50.2 | 58.5 | 72.7 |

[a] **I:** CCSD(T)/Lanl2dz//B3LYP/Lanl2dz. **II:** CCSD(T)/[6-31G(d,p)+Lanl2dz]//B3LYP/[6-31G(d,p)+Lanl2dz]. [b] The experimental values are obtained based on the heats of formation at 0 K for $(CH_3)_3In$ = 52.97 kcal/mol (calculated from 298 K value given in (ref 18a) using vibrational frequencies in this work); $H_2O$= −57.127 kcal/mol (ref 18b); $H_2S$= −4.204 kcal/mol (ref 18b); $CH_4$= −16.0 ± 0.08 kcal/mol (ref 18b); $CH_3$ = 35.86 ± 0.07 kcal/mol (ref 24); experimental values of InO (88.72, 10.72, ≤37.7 kcal/mol) and InS (57.36 kcal/mol).

(−4.20 kcal/mol).[18b,19] The heat of formation is calculated using the general formula given below,

$$\Delta_f H_0^\circ((CH_3)_3In{:}OH_2) = \Delta_f H_0^\circ((CH_3)_3In) + \Delta_f H_0^\circ(H_2O) + \Delta_r H_0^\circ \quad (5)$$

The heats of reaction calculated at CCSD(T)/Lanl2dz//B3LYP/Lanl2dz level are −15.95 and −5.17 kcal/mol, respectively, for the $H_2O$ and $H_2S$ reactions. The predicted heat of formation $\Delta_f H_0^\circ$ (0 K) of the $(CH_3)_3In{:}OH_2$ is −20.13 kcal/mol and that of $(CH_3)_3In{:}SH_2$ is 43.60 kcal/mol. The predicted heats of formation for $(CH_3)_2InOH$, $(CH_3)_2InSH$, $CH_3InO$ and $CH_3InS$ are −20.63, 31.79, 29.04, and 48.41 kcal/mol, respectively. The corresponding experimental values are not available. The data are summarized in Table 5.

In the case of InO, the dissociation energy ($D_0^\circ$) reported by different methods differ greatly. First, Howell determined the dissociation energy ($D_0^\circ$) of InO radical to be 25 kcal/mol using spectroscopic data.[20] Gurvich et al. gave the $D_0^\circ$ value as 103 kcal/mol using the thermochemical measurements in flames.[21] Later the third-law analysis by Brewer et al. gave an upper limit for the dissociation energy of InO as ≤76 kcal/mol.[22] So clearly the spectroscopic value is too low when compared to other oxides; on the other hand, the flame result appears to be too high. For this, the upper limit of $D_0^\circ(InO) = 76$ kcal/mol tends to support the latter value and the identification of $InO^+$ as a parent ion.[8] The heat of formation for InO can be found from the relationship

$$D_0(In - O) = \Delta_f H_0^\circ(In) + \Delta_f H_0^\circ(O) - \Delta_f H_0^\circ(InO) \quad (6)$$

The heats of formation of indium atom and oxygen atom are 54.7 and 59.0 kcal/mol, respectively, at 0 K taken from NIST-JANAF tables.[19,23] On the basis of the above relationship, the three $D_0^\circ$ values of the spectroscopic, flame and third-law analysis methods give the heats of formation of InO as 88.7, 10.7 and ≤37.7 kcal/mol respectively. Experimentally, the heat of formation for InS is available as 55.7 kcal/mol at 298 K.[24] The corresponding value at 0 K, $\Delta_f H_0^\circ = 57.4$ kcal/mol, calculated using the $[H^\circ(0) - H^\circ(298.15\ K)]$ value −2.37 kcal/mol and the standard reference states of $In_{(s)}$ and $S_{(s)}$, 1.85 and 2.18 kcal/mol, respectively.[19,23] Our predicted heats of formation of InO and InS at 0 K listed in Table 5, 35.5, and 58.5 kcal/mol, are in good agreement with the values derived from experimental data, ≤37.7 and 57.4 kcal/mol, respectively, cited above.

## Conclusions

The reaction mechanisms for the combination of the $(CH_3)_3$-In with $H_2O$ and $H_2S$ reactions have been investigated by DFT (B3LYP) and ab inio (MP2) methods. First the reactions proceed via molecular complexes with 12.6 and 3.9 kcal/mol binding energy to form $(CH_3)_3In{:}OH_2$ (**R1**) and $(CH_3)_3In{:}SH_2$ (**R2**). These complexes can dissociate to produce different products via different transition states. The transition states for the productions of $(CH_3)_2InOH$, $(CH_3)_2InSH$, $CH_3InO$ and $CH_3InS$ lie above the reactants at 7.3, 18.2, 39.4 and 24.2 kcal/mol, respectively. Finally, the intermediates $CH_3InX$ (X = O, S) decompose into InO, InS and $CH_3$ radicals, and the energies required for the reactions is 48.0 and 50.2 kcal/mol respectively. Based on the CCSD(T)/Lanl2dz//B3LYP/Lanl2dz and CCSD-(T)/[6-31G(d,p)+Lanl2dz]//B3LYP/[6-31G(d,p)+Lanl2dz] level of theory, we can calculate the heats of reaction and heats of formation. The predicted heats of formation for $(CH_3)_2InOH$, $(CH_3)_2InSH$, $CH_3InO$ and $CH_3InS$ are −20.6, 31.8, 29.0 and 48.4 kcal/mol respectively. From these reactions we calculated the heats of formation of InO and InS at 0 K 35.5 and 58.5 kcal/mol. These values are in reasonable agreement with the experimental heats of formation of $\Delta_f H_0^\circ$ of InO, ≤ 37.7 kcal/mol, and InS, 57.4 kcal/mol.

We have also studied the reactions of $H_2O$ and $H_2S$ of $(CH_3)_2$-In, which may be present in CVD experiments using heated reactors. Both reactions were found to occur via the association-$CH_4$ elimination mechanisms similar those of the TMIn reactions. The most stable intermediates of the reactions are $CH_3InXH$ (X = O, S), both of them undergo $CH_4$-elimination by $CH_3$ migration producing novel $InXH{:}CH_3$ molecular complexes prior their fragmentation to InX + $CH_4$.

The results presented in this study suggest that for the deposition of InO and InS thin films by OMCVD or PECVD using TMIn and $H_2X$, stable intermediates such as $(CH_3)_2InXH$ and $CH_3InXH$ can be readily formed in the upstream before they reach a heated substrate. Their interactions with the substrate may give rise to InX readily by surface catalytic reactions. The reaction TMIn and $H_2S$ on $TiO_2$ surface might have vastly different barriers than those calculated here.

**Acknowledgment.** The authors thank the Institute of Nuclear Energy Research (INER), Taiwan, for the funding of this project. M.C.L. acknowledges the support from the Taiwan Semiconductor Manufacturing Company for the TSMC Distinguished Professorship and for the National Science Council of Taiwan for the Distinguished Visiting Professorship at National Chiao Tung University in Hsichu, Taiwan.

**Supporting Information Available:** Moments of inertia, vibrational frequencies, and bonding energies. This material is available free of charge via the Internet at http://pubs.acs.org.

## References and Notes

(1) Barron, A. R. *Adv. Mater. Opt. Electron.* **1995**, *5*, 245.

(2) Kim, W.-T.; Kim, C.-D. *J. Appl. Phys.* **1986**, *60*, 2631.

(3) Gasanly, N. M.; Aydinli, A. *Solid State Commun.* **1997**, *101*, 797.

(4) Asikainen, T.; Ritala, M.; Leskela, M. *Appl. Surf. Sci.* **1994**, *82/83*, 122.

(5) (a) Rehwald, W.; Harbeke, G. *J. Phys. Chem. Solids* **1965**, *26*, 1309. (b) Ott, A. W.; Johnson, J. M.; Klaus, J. W.; George, S. M. *Appl. Surf. Sci.* **1997**, *112*, 205. (c) Ozasa, K.; Ye, T.; Aoyagi, Y. *Thin Solid Films* **1994**, *246*, 58. (d) Calixto-Rodriguez, M.; Tiburcio-silver, A.; Ortiz, A.; Sanchez-juarez, A. *Thin. Solid Films* **2005**, *133*, 480−481.

(6) (a) O'Brien, P.; Otway, D. J.; Walsh, J. R. *Thin. Solid Films* **1998**, *315*, 57. (b) Seyam, M. A. M. *Vacuum* **2001**, *63*, 441. (c) Hogg, J. H. C.; Duffin, W. G. *Phys. Status Solidi* **1966**, *18*, 755. (d) Nishino, T.; Taniguchi, K.; Hamakawa, Y. *Solid State Commun.* **1976**, *19*, 635. (e) Nishino, T.; Taniguchi, K.; Hamakawa, Y. *Jpn. J. Appl. Phys.* **1974**, *13*, 1921.

(7) (a) Watson, W. W.; Shambon, A. *Phys. Rev.* **1936**, *50*, 607.

(8) Burns, R. P.; Demaria, G.; Drowart, J.; Inghram, M. G. *J. Chem. Phys.* **1963**, *38*, 1035.

(9) Srivastava, R. D.; Farber, M. *Chem. Rev.* **1978**, *78*, 627.

(10) Granqvist, C. G. *Appl. Phys. A* **1993**, *57*, 19.

(11) (a) Cardelino, B. H.; Moore, C. E.; Cardelino, C. A.; Frazier, C. A.; Bachmann, K. J. *J. Phys. Chem. A* **2001**, *105*, 849. (b) Rothschopf, G. K.; Perkins, J. S.; Li, S.; Yang, D.-S. *Phys. Chem. A* **2000**, *104*, 8178. (c) Himmel, H.-J.; Downs, A. J.; Greene, T. M. *J. Am. Chem. Soc.* **2000**, *122*, 9793. (d) Tachikawa, H.; Kawabata, H. *J. Mater. Chem.* **2003**, *13*, 1293. (e) Nakamura, K.; Makino, O.; Tachibana, A.; matsumoto, K. *J. Organomet. Chem.* **2000**, *611*, 514.

(12) Frisch, M. J.; Trucks, G. W.; Schlegel, H. B.; Scuseria, G. E.; Robb, M. A.; Cheeseman, J. R.; Montgomery, Jr. J. A.; Vreven, T.; Kudin, K. N.; Burant, J. C.; Millam, J. M.; Iyengar, S. S.; Tomasi, J.; Barone, V.; Mennucci, B.; Cossi, M.; Scalmani, G.; Rega, N.; Petersson, G. A.; Nakatsuji, H.; Hada, M.; Ehara, M.; Toyota, K.; Fukuda, R.; Hasegawa, J.; Ishida, M.; Nakajima, T.; Honda, Y.; Kitao, O.; Nakai, H.; Klene, M.; Li, X.; Knox, J. E.; Hratchian, H. P.; Cross, J. B.; Adamo, C.; Jaramillo, J.; Gomperts, R.; Stratmann, R. E.; Yazyev, O.; Austin, A. J.; Cammi, R.; Pomelli, C.; Ochterski, J. W.; Ayala, P. Y.; Morokuma, K.; Voth, G. A.; Salvador, P.; Dannenberg, J. J.; Zakrzewski, V. G.; Dapprich, S.; Daniels, A. D.; Strain, M. C.; Farkas, O.; Malick, D. K.; Rabuck, A. D.; Raghavachari, K.; Foresman, J. B.; Ortiz, J. V.; Cui, Q.; Baboul, A. G.; Clifford, S.; Cioslowski, J.; Stefanov, B. B.; Liu, G.; Liashenko, A.; Piskorz, P.; Komaromi, I.; Martin, R. L.; Fox, D. J.; Keith, T.; Al-Laham, M. A.; Peng, C. Y.; Nanayakkara, A.; Challacombe, M.; Gill, P. M. W.; Johnson, B.; Chen, W.; Wong, M. W.; Gonzalez, C.; Pople, J. A. *Gaussian 03*, Revision C.02; Gaussian, Inc., Wallingford CT 2004.

(13) (a) Becke, A. D. *Phys. Rev. A.* **1998**, *38*, 3098. (b) Lee, C.; Yang, W.; Parr, R. G. *Phys. Rev. B* **1988**, *37*, 785. (c) Becke, A. D. *J. Chem. Phys.* **1993**, *98*, 5648.

(14) (a) Dunning, T. H. Jr.; Hay, P. J. In *Modern Theoretical Chemistry*; Schaefer, H. F., III, Ed.; Plenum Press: New York; 1977. (b) Hay, P. J.; Wadt, W. R. *J. Chem. Phys.* **1985**, *82*, 270. (c) Wadt, W. R.; Hay, P. J. *J. Chem. Phys.* **1985**, *82*, 284. (d) Hay, P. J.; Wadt, W. R. *J. Chem. Phys.* **1985**, *82*, 299.

(15) (a) Gonzalez, C.; Schlegel, H. B. *J. Chem. Phys.* **1989**, *90*, 2154. (b) Gonzalez, C.; Schlegel, H. B. *J. Phys. Chem.* **1990**, *94*, 5523.

(16) (a) Cizek, J. *Adv. Chem. Phys.* **1969**, *14*, 35. (b) Purvis, g. D.; Bartlett, R. J. *J. Chem. Phys.* **1982**, *76*, 1910. (c) Scuseria, G. E.; Janssen, C. L.; Schaefer, H. F., III. *J. Chem. Phys.* **1988**, *89*, 7382. (d) Scuseria, G. E.; Schaefer, H. F., III. *J. Chem. Phys.* **1989**, *90*, 3700. (e) Boys, S. F.; Bernardi, F. *Mol. Phys.* **1970**, *19*, 553.

(17) (a) Schwerdtfeger, P.; Dolg, M.; Schwarz, W. H.; Bowmaker, G. A.; Boyd, P. D. W. *J. Chem. Phys.* **1989**, *91*, 1762. (b) Andrae, D.; Haubermann, U.; Dolg, M.; Stoll, H.; Preuss, H. *Theor. Chim. Acta* **1990**, *77*, 123. (c) Bergner, A.; Dolg, M.; KYchle, W.; Stoll, H.; Preuss, H. *Mol. Phys.* **1993**, *80*, 1431.

(18) (a) Clark, W. D.; Price, S. J. *Can. J. Chem.* **1968**, *46*, 1633. (b) NIST Standard Reference Database Number 69, which can be accessed electronically through the NIST Chemistry Web Book (http://webbook/nist/gov/chemistry/).

(19) Chase, M. W. Jr.; Davies, C. A.; Downey, J. R. Jr.; Frurip, D. J.; McDonald, R. A.; Syverud, A. N. JANAF Thermochemical Tables. *J. Phys. Chem. Ref. Data* **1985**, *14*, Suppl. 1.

(20) Howell, H. G. *Phys. Soc. (London)* **1945**, *57*, 32.

(21) Gurvich, L. V.; Veits, I. V. *Izv. Akad. Nauk. SSSR. Ser. Fiz.* **1958**, *22*, 673.
(22) Brewer, L.; Chandrasekhariah, M. S. *UCRL-8713 (Rev.*) 1960.
(23) Pankratz, L. B. *Thermodynamic Properties of Elements and Oxides*; Bureau of Mines Bulletin 672; U.S. Department of the Interior: Washington, DC, 1982.
(24) (a) Barin, I. *Thermochemical Data of Pure Substances*; VCH: Weinheim, Germany, 1989. (b) In *CRC Handbook of Chemistry and Physics*, 60th ed.; Weast, R. C., Ed.; CRC Press: Boca Raton, FL, 1980.
(25) Ruscic, B.; Litorja, M.; Asher, R. L. *J. Phys. Chem. A* **1999**, *103*, 8625.